Pergamon

Energy Convers. Mgmt Vol. 38, No. 2, pp. 131–149, 1997

PII: S0196-8904(96)00015-5
0196-8904/97 $15.00 + 0.00

APPLICATION OF SURGE ARRESTERS FOR THE PROTECTION OF SF_6 SUBSTATIONS

ABDEL-SALAM H. A. HAMZA
Electrical Engineering Department, Faculty of Engineering, Shoubra, Cairo, Egypt

(Received 29 April 1995)

Abstract—Sulphur hexafluoride (SF_6) gas-insulated substations (GIS) are exposed to the same types of overvoltages as conventional substations, such as lightning overvoltages, switching overvoltages and temporary overvoltages. Possible means to limit overvoltages in a GIS are active gap (SiC) surge arresters and metal oxide (ZnO) surge arresters. The objective of this work is to study the effects of the system configuration on the performance of these two types of overvoltage limiting devices. The results obtained from the study are presented and discussed, and some general conclusions are suggested. Copyright © 1996 Elsevier Science Ltd

Electrical power systems Gas insulated substation Protection Surge arresters

1. INTRODUCTION

Transients causing overvoltages occur in the system due to different causes, and the peak values of these can be much in excess of the operating voltage. Because of this, an area of critical importance in the design of power systems is the consideration of the insulation requirements for lines, cables and stations. Also, devices must be provided to protect items of the plant that may have different breakdown levels and different voltage–time (V–t) characteristics. In order that all items of the system be adequately protected, there is a need to consider the situation as a whole. In particular, the system engineer has to consider the following three topics, which constitute the general problem of insulation coordination (an important procedure for the provision of a safe, efficient, and reliable transmission and/or distribution system):

(i) the origins and properties of surges and overvoltages;
(ii) the insulation characteristics of the equipment; and
(iii) the limitation of surges by surge arresters.

Three types of overvoltages can occur in power system networks: lightning, switching and temporary (or dynamic) overvoltages. Within each of these categories, there exists an extremely wide variety of phenomena, determined in part by the various causes of overvoltages and in part by the different possible network configurations and the various switching and operating conditions.

In the case of lightning, the overvoltages can occur through a direct stroke or be induced through a back-flashover. Lightning has been studied for many years, and volumes of data, as well as numerous theories about its occurrence, effect, and control, have been produced [1–3].

A lightning surge can be represented as a difference of exponentials by the following [4]:

$$e = E(e^{-\alpha t} - e^{-\beta t}) \tag{1}$$

where α and β are constants (they determine the waveshape) and E determines the magnitude of the lightning represented as a voltage surge.

1.1. Objective of the study

Technical progress in the following two areas has been primarily responsible for a new impetus in the field of insulation coordination: the increasing use of gas-insulated substations (GIS) and the development of zinc oxide (ZnO) surge arresters. The entirely different behaviour of the new

types of insulation used in the GIS, in comparison with conventional air insulation, requires a new approach to the problem of protection against transients. Since the damage in the case of failure is more extensive, the acceptable risk must be lower. Surge arresters of the purely solid-state ZnO types work in a different mode of operation than conventional ones. Accordingly, new testing procedures and standards have to be established, based on extensive studies of the systems to be protected and on the characteristics of these new devices.

The aim of this study is to investigate the possible overvoltages occurring in sulphur hexafluoride (SF_6)GIS as a result of a lightning stroke and to study the effects of the system configuration on the performance of two types of surge arresters: the current limiting conventional arrester and the more recent zinc oxide (or metal oxide) arrester.

1.2. SF_6 GIS characteristics

The first characteristic necessary for designing a coaxial metal-clad busbar is the dielectric behavior, which depends on the diameters of the conductor and the encapsulation. These two diameters shall be such that the electric field at the conductor surface is less than a maximum value that depends on the pressure of the SF_6 inside the encapsulation and on the surface condition of the busbar and the cladding. Because the gas-insulated system is totally enclosed, there is an economic advantage in reducing the size of the enclosure at the expense of higher electrical gradients in the internal insulation. Therefore, the voltage stresses must be determined carefully to ensure an optimum balance between insulation level and economics is achieved.

The wave propagation and, thus, the occurring overvoltages depend on the surge impedance of the GIS. This can be obtained by one of two formulas [5, 6]:

$$Z = 60 \ln\left(\frac{r_2}{r_1}\right) \tag{2}$$

or

$$Z = \left(\frac{138}{\sqrt{k}}\right) \log_{10}\left(\frac{r_2}{r_1}\right) \tag{3}$$

where Z is the surge impedance in Ω, r_2 is the inner radius of the outer sheath, r_1 is the radius of the inner conductor and k is the permittivity of the dielectric, which is unity for SF_6. For an optimum system, the surge impedance is exactly 60 ohms. Due to the small variation of the dimensions from the optimum of the insulation, only a moderate variation between 55 and 100 ohms can be found for all voltage ranges [5].

One of the major advantages of the GIS is their compact size. Representative gas-insulated systems occupy approximately 1/25 of the volume and 1/10 of the area of a conventional open-air substation [7]. The typical GIS with its compactness has bus runs between various pieces of equipment that are much shorter than in a conventional substation. These lengths are directly related to the system voltage. Generally, the lower the voltage level, the shorter are the bus runs. The difference in surge impedance between different parts of a GIS is usually limited: the coefficient of refraction only slightly deviates from unity. For insulation coordination purposes, the influence of the different apparatus can often be neglected and regarded as an extra safety margin [5]. In general, the wave propagation velocity of a GIS is comparatively slow with respect to conventional substations. In the case of SF_6 gas-insulated equipment, the ratio of the Basic Switching Impulse Insulation Level (BSL) to the Basic Lightning Impulse Insulation Level (BIL) is close enough to unity and a BSL/BIL ratio equal to 1 can be used for gas insulated systems. Another advantage of a GIS is the absence of atmospheric contamination on insulating surfaces, thus reducing the frequency of occurrence of flashovers. Metal-clad substations, built originally to solve the problems of size and environment, now enable the constant increase in fault currents to be met in an elegant way [8]. In addition to the advantages mentioned, due to a perfect metal casing, atmospheric effects are negligible, which improves the insulation quality considerably [9]. The introduction of new technologies and new components, such as the gas circuit breaker [10] and the ZnO arresters, promote the introduction of the GIS. The near future will probably see the development of three phase enclosure type GIS as integrated systems including these new components and technologies.

The reduction in size and volume saves not only installation space, but also materials, and reduces the number of arresters required. A decrease in the number of sealings contributes reduced probability of leakage and, hence, increased reliability of the system. It also makes the maintenance of a GIS easy, which, in any case, is less crucial than for conventional substations.

1.3. Surge arresters

One of the means of protecting transmission equipment is the surge arrester. Two types of surge arresters may be used for this reason: active gap (SiC) and gapless (ZnO) metal oxide surge arresters.

1.3.1. Active gap (SiC) arrester. The two principal components of active gap surge arresters (diverters) are the spark gap and the non-linear resistor. One of the earlier designs was the lightning arrester with plate gaps, which is still used today in some medium voltage networks. At still higher voltages, arresters with magnetically blow spark gaps are more commonly used, in particular in EHV networks (300–750 kV). These consist mainly of three parts: spark gaps, discharge resistors and a grading system that monitors the distribution of voltage across the spark gaps.

Much literature has been published about current limiting gap characteristics [11–14]. A v–t curve for the voltage across the gaps after sparkover can be described as follows. At first, there is a very low constant voltage for a period of 100–300 μs or more during which the arc is developing. This is followed by a rapid voltage rise as the arc is being extended. The crest value of this voltage depends on the current rise time and magnitude and on the design of the arc chambers. It may range from 0.3 to 0.85 pu of peak arrester rating [15]. Finally, the arc voltage starts to decay after a short period because of heating of the insulating material, the rate of decay being a function of absorbed energy. The spark gap characteristic is represented in this study as described by Carrara *et al.* [11].

The second important active element of active gap arresters is the discharge resistor. It has to satisfy two conflicting requirements. At heavy surge currents, it should present a relatively low resistance, thus enabling heavy current overvoltages to be limited to values below the withstand level of the protected equipment when sparkover occurs. On the other hand, it has to help limit the subsequent power frequency current in order that the spark gaps may interrupt it. These two requirements are satisfied by non-linear resistors. In gapped surge arresters, they are usually made of silicon carbide (SiC). The non-linear characteristics can be expressed by the function

$$I = k' V^{\delta} \tag{4}$$

where k' is a constant depending on the resistor block dimensions and δ is the non-linearity constant and approaches 5 [15].

1.3.2. Zinc oxide arresters. The materials used for ZnO arresters are uniformly mixed, formed into grains, and sintered through special processes at temperatures between 1100 and 1350°C [16, 17]. The gapless surge arrester obtained using ZnO elements has the property that its resistance decreases sharply as the voltage across it increases. Therefore, its voltage–current characteristic, for practical purposes, is usually expressed in the following form [18, 19]:

$$V = KI^{\beta} \tag{5}$$

where V is the instantaneous voltage across the arrester, I is the current flowing through it and K is a constant of the arrester and varies mainly with the physical dimensions of the material. β is the characteristic index of the arrester (the non-linearity exponent constant) and is determined by the type of material used, its impurity content and crystal size. The value of β for ZnO materials is around 0.02–0.1. The resultant value of K is determined by the number of arrester discs connected in series or in parallel. If n identical discs are connected in series, the resultant constant will be,

$$K_{\text{effective}} = nk \tag{6}$$

where k is the disc unit constant and $K_{\text{effective}}$ is the arrester (of n units) constant. In case of parallel connection of the same discs, the current density is reduced n times and the constant is decreased by n^{β} [18]:

$$K_{\text{effective}} = k/n^{\beta} \tag{7}$$

Equation (4) may be re-written in the following form [4, 18]:

$$I = K_1 V^{\alpha} \tag{8}$$

where K_1 is constant and $\alpha(=1/\beta)$ is the non-linear constant, which is generally defined by

$$\alpha = \frac{\log I_2 - \log I_1}{\log V_2 - \log V_1} \tag{9}$$

for two known points on the V–I characteristic curve. In order to keep the stress on the system insulation as low as possible, a good overvoltage protection system or, on the other hand, an arrester has to meet and fulfil the following requirements [20, 21]:

(i) it must withstand the normal phase to earth voltage of the system for the whole of its operating life, even in the presence of pollution and after repeated discharges of high energy, such as are expected in a network;
(ii) it must withstand, without damage, temporary overvoltages caused by earth faults and other system transient conditions and discharge these overvoltages to earth without causing an earth fault;
(iii) interruption of the following current;
(iv) the energy absorption capability must be such that, even after the most severe switching surges and temporary overvoltages, the temperature of the blocks does not rise to a point where thermal runaway sets in;
(v) protection level must be maintained as low as possible.

The newly developed ZnO surge arrester with its excellent high non-linearity characteristic, energy capability and protective performance can meet these conditions and fulfil these requirements.

2. INVESTIGATIONS AND RESULTS

The effects of different factors on the overvoltages produced on the SF_6 GIS, with active gap (SiC) arresters and gapless metal oxide (ZnO) arresters connected for protection, are investigated using a computer program, which simulates the different system configurations, and different variables are calculated (such as the voltages at different points on the system, arrester stresses (currents and energies)). The various circuit configurations considered consist mainly of a single three-phase compressed gas-insulated bus-duct connected to an overhead transmission line (OHL) at one end and open circuited at the other. Both the overhead line and the GIS feeder or bus assume various lengths. Also, a cable of varying length is connected between the overhead line and feeder. Alternatively, a transformer represented by its surge capacitance to earth is connected at the feeder open end, as is the case in most substations. Finally, with the transformer at the open end, a cable is added, either between the OHL and feeder or between the feeder and transformer. Cases are also considered, however, with an OHL between the feeder and transformer.

The overvoltages considered originated from a lightning stroke terminating on phase "a" of the OHL. Different waveshapes and magnitudes are considered, which could simulate either shielding failures or back-flashovers. Surge arresters, either active gap silicon carbide (SiC) or gapless metal oxide (ZnO), are connected at different points on the circuits, usually at the entrance of the GIS. The different data used for the investigations are given in the Appendix. The cases of study included are shown below.

2.1. Effect of GIS length

One of the most important aspects in insulation coordination of a GIS is perhaps the influence of its own length upon the overvoltages. Figure 3 shows the effect of varying the GIS length (L) in the system configuration of Figs 1 and 2 with an active gap (SiC) arrester connected at the GIS entrance. It can be seen that the longer the GIS, the higher are the overvoltages. The results shown correspond to the system configuration when the power source is a simulated inductive generator or an infinitely long line (this means that no reflections from the source can influence the voltage variations). From this, there would seem to be an optimum length between 173.4 and 260.1 m, which would constitute a worst case. As seen in Fig. 3, the voltage at the GIS entrance (arrester

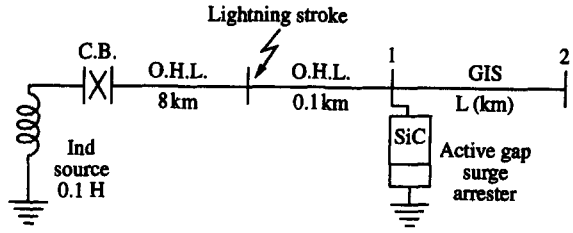

Fig. 1. System under study.

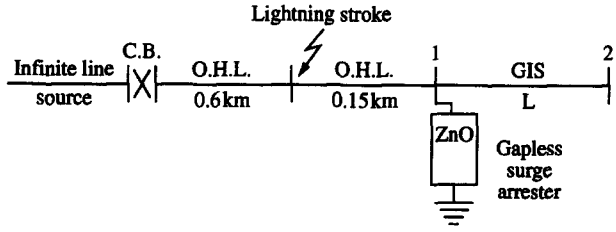

Fig. 2. System under study.

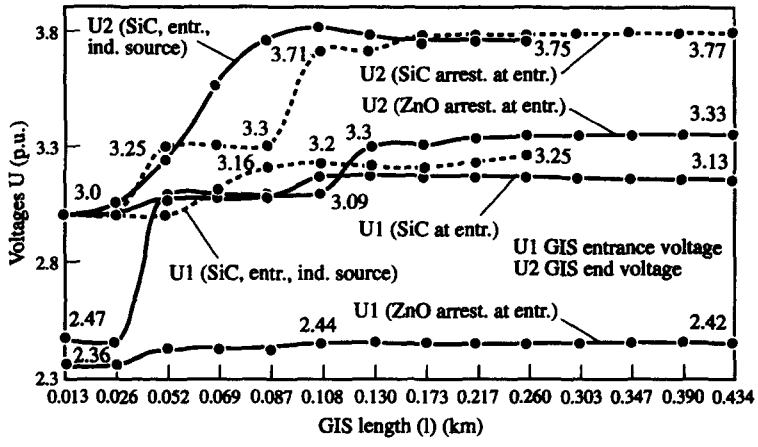

Fig. 3. Effect of GIS length on the overvoltages with arrester connected at its entrance (ind. and infinite line source).

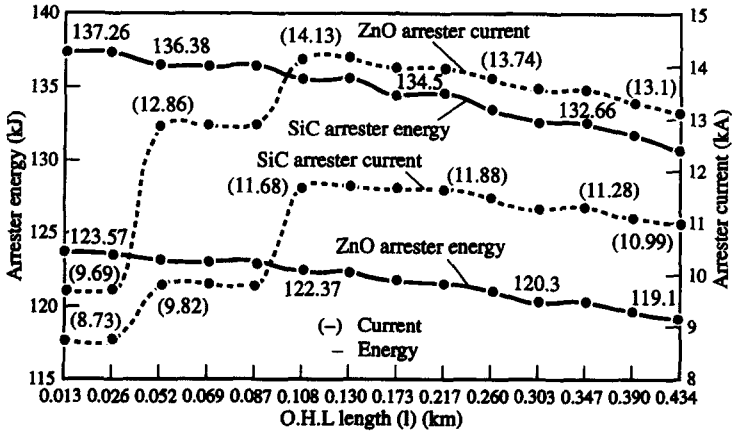

Fig. 4. Effect of the GIS length on the arrester current and energy, an arrester connected at the GIS entrance (infinite line source).

location) initially increased with the GIS length, but then it started to decrease again for lengths beyond 260.1 m. From Fig. 4, the peak current through the arrester shows the same trend, while the voltage at the GIS open end does not show any further increase beyond 3.77 pu for GIS lengths greater than 173.4 m. This corresponds to an overvoltage of 1231.28 kV. The lightning waveshape used for calculations in most of this work is based upon the standard 1.2/50 μs definition, except where otherwise specified. It would probably be worthy to investigate further the effect of varying GIS length in the case of lightning surges of different durations, as the build-up time of overvoltages and, therefore, the superposition of reflected and incident waves are affected by both factors. Comparison of the results in Fig. 3, for inductive source and infinite line source systems, suggests that reflections from nearby inductive sources only have an adverse effect for GIS lengths greater than about 86.7 m. Assuming a standard insulation level of 1300 kV, the station could, therefore, be found at this point to be protected effectively with a single surge arrester at the GIS entrance. It might be interesting to note the extent to which the lightning arrester modifies the overvoltage conditions by comparing the values of the overvoltages produced at the GIS entrance and end without a surge arrester (for Fig. 2 system), which are found to be 10.88 and 10.89 pu, respectively, with that when an arrester is allocated, which are 3.07 and 3.3 pu, respectively (for the GIS length of 87 m). These concern a possibly worst-case GIS length of 86.7 m (in practice, GIS lengths rarely exceed 100 m) with and without an arrester.

The calculations are made for a voltage duration of 100 μs in most cases. The calculations concerning the energies absorbed by arresters are cumulative. It is, thus, seen from Fig. 4 that the total energy absorbed over a period of about 100 μs decreased as the GIS length increased. However, it is also noted from the computer output, that some "follow" current (of the order of less than 100 A) is still flowing through the arrester at that time. This "residual" current increased with the GIS length. Therefore, the overall energy absorbed in each case over the period up to actual resealing of the arrester can be assumed to be comparatively equal for each case. Since the energy dissipation occurs over a longer time period, the reliability of arresters is somewhat improved by increased GIS length. The higher energies shown in Fig. 4, for the system shown in Fig. 1, are due to reflections from the source, causing a second sparkover of the arrester and postponing its resealing time to allow for more current to be diverted to earth.

When a gapless metal oxide (ZnO) arrester is connected to the GIS entrance, as shown in Fig. 2, the results obtained are shown in Figs 3 and 4. The results show that the peak currents through the arresters are much higher than the case when an active gap (SiC) arrester is connected, but that effectively less energy has to be handled. This was confirmed by the residual currents at the end of the 100 μs period, which are observed to be lower. This can be explained since the active gap was set to sparkover at a level of 1.8 pu (587.88 kV), which introduces a time delay before the arrester can operate, whereas the gapless arrester starts to conduct a much higher current at a lower level. The result is that maximum overvoltages are lower, having been reduced to 3.33 pu (1087.57 kV).

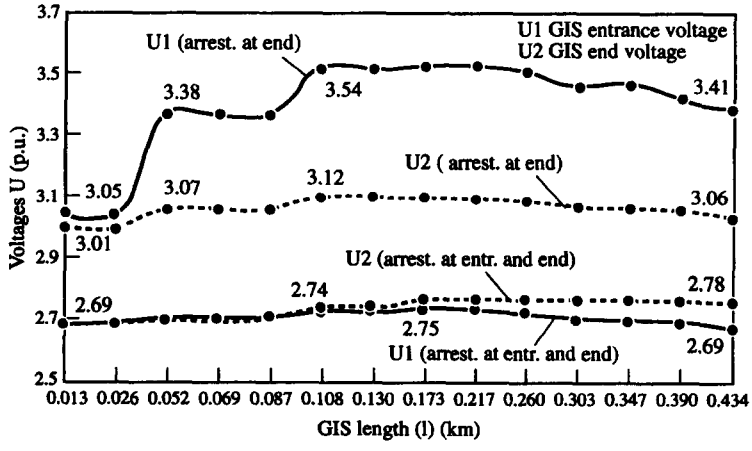

Fig. 5. Effect of GIS length on the overvoltages with SiC arrester connected at its ends (infinite line source).

Table 1. Effect of distance to lightning and GIS length on arresters current and energy with two active gap arresters connected at both GIS ends (inductive source)

Lightning distance (I_1) (km)	GIS length (I_2) (km)	Arrester 1 energy (kJ)	Arrester 1 current (kA)	Arrester 2 energy (kJ)	Arrester 2 current (kA)
0.35	0.013	97.5	5.0	97.5	5.0
	0.052	96.0	5.0	97.0	5.0
	0.087	96.0	4.9	97.0	5.25
1.4	0.013	112.5	4.9	112.5	4.9
	0.052	110.0	5.1	112.0	4.8
	0.087	105.0	5.3	111.5	5.25
3.5	0.013	135.0	5.0	135.0	5.0
	0.052	133.0	5.0	135.0	5.0
	0.087	127.0	5.25	134.0	5.3

A better protection as well as a higher reliability of service is, therefore, afforded by gapless ZnO arresters. Otherwise, the same general effects of varying GIS length appear in Figs 3 and 4.

Figure 5 shows the resulting overvoltages of when, in the system shown in Fig. 2, an active gap surge arrester is connected at the GIS open end only. The highest overvoltages (3.54 pu, i.e. 1156.16 kV) occur at the GIS entrance and are somewhat lower than in the case when the arrester is at the GIS entrance. The peak currents are also somewhat lower. Thus, an even better protection can be expected with a gapless ZnO arrester at the GIS open end. The effect of varying the GIS length is the same as that observed for the systems in Fig. 2, with the exception that, for a system with an arrester at the open end, the voltages decrease at both GIS ends as its length is increased beyond 260.1 m, instead of just at its entrance. It would appear, therefore, that placing an arrester at the GIS end only is worth considering, although connections to the OHL, which might have weaker insulation than other parts, would have to be considered carefully.

When an active gap surge arrester is located at both GIS ends for the same system, the maximum overvoltage of 2.78 pu (907.94 kV) occurs at the open end, as can be seen in Fig. 5. It should be mentioned, however, that, as the incoming surge is short-circuited at both ends of the GIS, there is a possibility that the highest overvoltages could occur at different points inside the GIS. As regards the absorbed energies, increasing the GIS length causes the initially equal sharing of current between the two arresters to shift towards a greater duty requirement for the open-end arrester, rather than at the GIS entrance. The voltage variations again show the same pattern as in Fig. 3. The above findings are also confirmed by the results of Tables 1 and 2.

2.2. Effect of distance to lightning stroke

Table 1 for the system in Fig. 6 and Table 2 for the same system, with only an arrester at the GIS entrance, demonstrate that, in the presence of reflections from a nearby power source, the energy requirements of arresters are significantly increased as the distance of a lightning stroke

Table 2. Effect of lightning distance and GIS length on GIS overvoltages with an active gap arrester at GIS entrance (0.1 H inductive source)

GIS length (I_2) (km)	Lightning distance (km)	Entrance voltage (U_1) (pu)	End voltage (U_2) (pu)	Arrester energy (kJ)	Arrester current (kA)
0.013	0.35	3.1	3.1	207	9.5
	0.70	3.1	3.1	216	9.5
	1.40	3.1	3.1	235	9.5
	2.40	3.05	3.1	255	9.4
	3.50	3.1	3.0	272	9.6
0.052	0.35	3.1	3.25	205	9.5
	0.70	3.15	3.0	214	9.55
	1.40	3.05	3.25	232	9.4
	2.40	3.1	3.1	251	10.0
	3.50	3.1	3.1	270	9.9
0.087	0.35	3.25	3.75	200	12.2
	0.70	3.22	3.75	210	11.75
	1.40	3.25	3.8	224	11.75
	2.40	3.27	3.8	248	12.1
	3.50	3.25	3.8	262	11.7

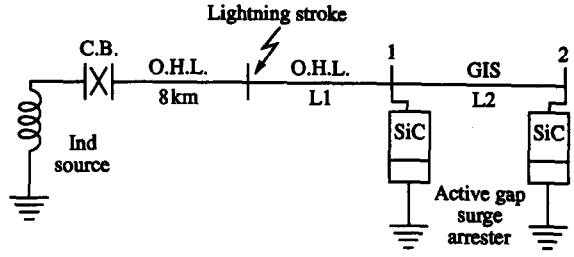

Fig. 6. System under study.

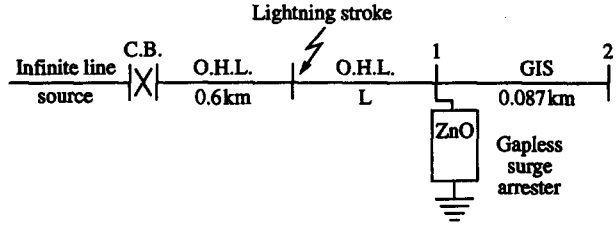

Fig. 7. System under study.

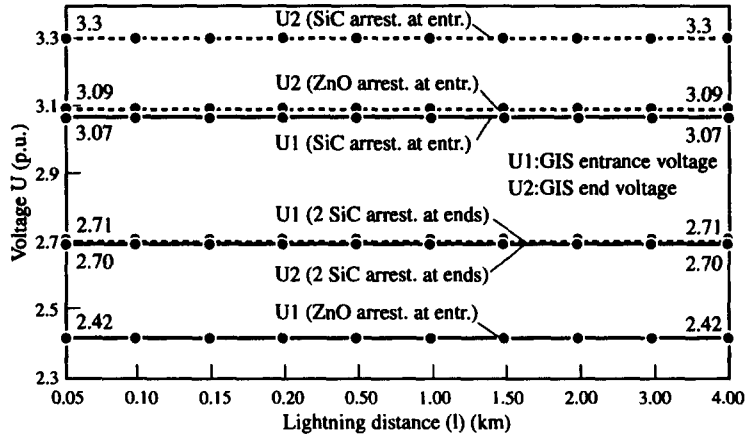

Fig. 8. Effect of distance to lightning stroke on GIS overvoltages arresters connected at GIS ends (infinite line source).

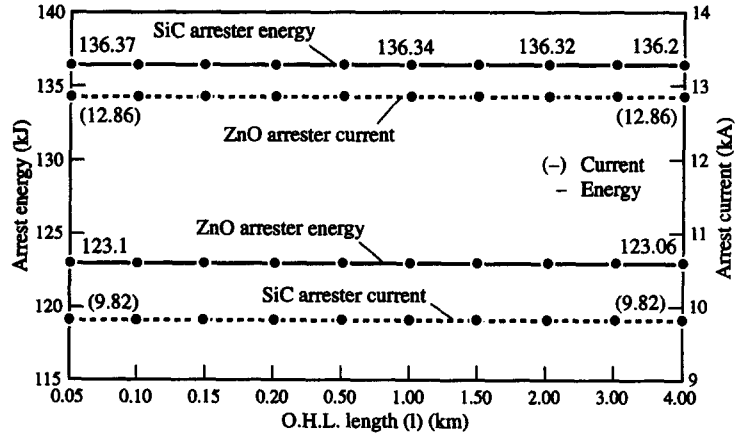

Fig. 9. Effect of the lightning distance on the arrester energy and current, an arrester connected at the GIS entrance (infinite line source).

Table 3. Effect of the source type on the GIS voltages and arrester stresses with an active gap (SiC) arrester connected at the GIS entrance

Source type	OHL length (l) (km)	Entrance voltage (U_1) (pu)	End voltage (U_2) (pu)	Arrester energy (kJ)	Arrester current (kA)
Inductive (0.1 H)	10	3.11	3.3	187.82	10.60
Inductive (0.1 H)	20	3.07	3.3	186.72	9.82
Infinite busbar	10	3.07	3.3	141.62	9.82
Infinite busbar	20	3.07	3.3	146.84	9.82
Infinite line	10	3.07	3.3	136.37	9.82
Infinite line	20	3.07	3.3	136.86	9.82

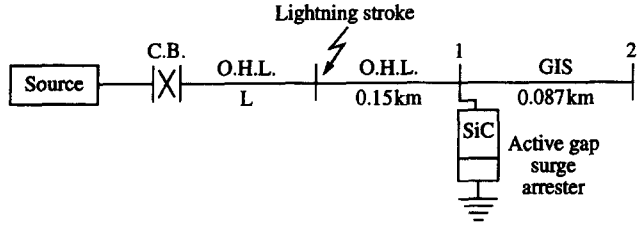

Fig. 10. System under study.

to the GIS entrance (L1) is increased, although this does not seem to affect overvoltage levels too significantly (the voltages at both GIS ends are found to be limited to 2.75 pu in all the cases of Table 1). In fact, Figs 8 and 9 show that overvoltages are very much unaffected by the distance from the GIS to the point of lightning stroke. For the results obtained in these figures, an active gap arrester or a gapless arrester at the GIS entrance and then an active gap arrester at both GIS ends are connected, respectively, to the systems shown in Fig. 7. The lack of reflections from a power source in these cases allowed for a slight decrease in energy absorption over the time period considered, as the lightning occurred further away from the GIS. However, it must be said that, as mentioned earlier, the losses and distortion caused by overhead transmission lines in practice, are not taken into account, and the calculations did not include the ensuing attenuations. In actual fact, the transmission line will limit the amplitude of overvoltages approximately to the line insulation level, and in addition, the wave steepness will be reduced due to corona. In practice, therefore, the severity of a lightning stroke is reduced by remoteness from the GIS, and only the closest back-flashovers (and eventual shielding failures) can be expected to cause concern.

2.3. Effect of source type

The results given in Table 3, for the system in Fig. 10, give a comparison for different types of source. The calculations concerning rows 1, 3 and 5, and rows 2, 4 and 6, are made for a voltage duration of 100 and 200 μs, respectively (to allow for reflections, since 3.336 μs $\times$ 20 km $\times$ 2 = 133.44 μs). Comparison of rows 1 and 2 shows that reflections from an inductive source can cause higher overvoltages than the original incoming surge if its distance from the GIS is less than perhaps 15 km, as suggested by the results shown in Table 4, for the same system. Conditions at the open end seem to be unaffected. Negative reflections from an infinite busbar also cause further

Table 4. Effect of source type and lightning distance from the source on the GIS voltages with an SiC arrester connected at its entrance

Source type	OHL (l) (km)	Entrance voltage (U_1) (pu)	End voltage (U_2) (pu)	Arrester energy (kJ)	Arrester current (kA)
Inductive (0.1 H)	7.85	3.2	3.75	190	11.7
Inductive (0.1 H)	15.85	3.2	3.75	187	11.75
Infinite bus	7.85	3.25	3.75	171	11.8
Infinite bus	11.85	3.2	3.75	186	11.75
Infinite bus	15.85	3.15	3.75	189	11.6
Infinite line	15.85	3.15	3.75	136	11.75

Table 5. Effect of the lightning waveshape on GIS voltages and arrester stresses with an arrester connected at GIS entrance (infinite line source)

Lightning waveshape (.../μs)	Active gap arrester (SiC)				Gapless arrester (ZnO)			
	U_1 (pu)	U_2 (pu)	Energy (kJ)	Current (kA)	U_1 (pu)	U_2 (pu)	Energy (kJ)	Current (kA)
0/1	2.97	3.24	7.36	8.07	2.37	3.23	6.61	10.14
0/5	3.17	3.81	42.88	11.78	2.43	3.35	38.64	13.97
0/50	3.21	3.87	395.81	12.84	2.45	3.37	353.06	15.04
0/100	3.23	3.88	863.8	12.95	2.45	3.38	725.69	15.16
1/5	3.07	3.18	40.27	9.87	2.41	3.01	35.26	12.71
1/50	3.09	3.33	398.33	10.16	2.42	3.01	354.64	13.23
1/∞	3.09	3.34	902.4	10.18	2.42	3.11	754.8	13.21
1.2/50	3.07	3.3	136.37	9.82	2.42	3.09	123.09	12.86

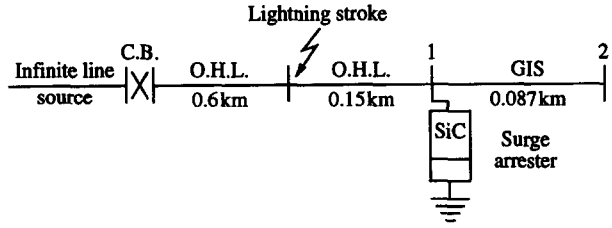

Fig. 11. System under study.

sparkover of the arrester, but they are not so severe as to affect maximum overvoltage levels, as shown in rows 3 and 4 of Table 3. Comparison of the energies absorbed in each case of Table 3 illustrates the effect of reflections. Table 3 gives a fairly general idea, but further investigation taking losses into account are required for analysis of such cases where small distances to an inductive source are involved, as may be the case for some industrial plants.

2.4. Effect of lightning characteristics

Table 5 shows the effect of lightning waveshape for the system shown in Fig. 11. The highest overvoltages are 3.88 pu (1103.9 kV) with a gapless ZnO arrester. They occur in the case of a

Table 6. Effect of lightning waveshape and magnitude and stroke distance on GIS voltages with an (SiC) active gap arrester connected at its entrance (inductive source)

Lightning waveshape (.../μs)	4 pu Volt ≅ 7.24 kA stroke, I = 0.5 km				6 pu Volt ≅ 10.86 kA stroke, I = 0.15 km			
	U_1 (pu)	U_2 (pu)	Energy (kJ)	Current (kA)	U_1 (pu)	U_2 (pu)	Energy (kJ)	Current (kA)
0/50	3.05	3.3	370	10.25	3.25	3.9	630	12.4
1/50	3.05	3.3	370	9.5	3.25	3.8	625	12.3
1.2/50	2.85	3.25	106	6.5	3.2	3.75	190	11.7

Table 7. Effect of the lightning stroke magnitude on GIS voltages and arrester stresses with an arrester connected at GIS entrance (infinite line source)

Lightning magnitude (pu/kA)	Active gap arrester (SiC)				Gapless arrester (ZnO)			
	U_1 (pu)	U_2 (pu)	Energy (kJ)	Current (kA)	U_1 (pu)	U_2 (pu)	Energy (kJ)	Current (kA)
4/7.24	2.81	2.89	73.3	5.85	2.31	2.63	68.18	10.33
5/9.04	2.93	3.02	103.55	7.53	2.37	2.9	95.18	10.33
6/10.85	3.07	3.3	136.37	9.82	2.42	3.09	123.09	12.86
7/12.66	3.19	3.58	171.85	12.32	2.45	3.24	152.22	15.2
8/14.47	3.29	3.83	208.95	14.78	2.48	3.36	182.34	17.42
10/18.09	3.46	4.25	287.92	19.57	2.53	3.53	244.94	21.61
12/21.71	3.58	4.59	372.18	24.17	2.58	3.67	310.03	25.63
14/25.32	3.69	4.88	460.81	28.6	2.61	3.77	377.08	29.55
16/28.94	3.78	5.13	553.16	32.91	2.65	3.86	445.74	33.41
20/36.18	3.94	5.53	747.26	41.26	2.7	4.0	586.95	41.01

Table 8. Effect of lightning stroke magnitude on the GIS ends overvoltages with an active gap (SiC) arrester at its entrance (0.1 H inductive source)

Lightning magnitude (pu volts/kA)	Entrance voltage U_1 (pu)	End voltage U_2 (pu)	Arrester energy (kJ)	Arrester current (kA)
6/10.86	3.2	3.75	190	11.7
8/14.48	3.55	4.4	289	16.9
20/36.18	4.0	6.0	945	44.5

0/100 μs wave. Comparison of the 0/100 μs and the 1/∞ waves shows that the steepness of the incoming surge is a more crucial factor than the wavetail. The steeper the front of the wave, the higher is the overvoltage, even if the tail is of shorter duration, since it builds up more rapidly. The higher energies are caused by the longer duration waves. The results shown in Table 6 (for the system shown in Fig. 6, with $L_2 = 0.087$ km and OHL = 7.85 km) lead to similar conclusions.

The effect of lightning magnitude is also investigated. Assuming an insulation of 1300 kV (3.98 pu) and allowing for a 20% BIL margin, as is usually the practice in insulation coordination, one should bear in mind that the preferred maximum overvoltage level is 1040 kV, i.e. about 3.18 pu. Various statistical studies have shown that the average lightning stroke has an average amplitude between 10 [2, 22] and 25 kA [23]. Table 7, for the system used with Table 5, shows that a metal oxide gapless arrester at the GIS connection is much preferable to an active gap arrester, especially if even higher lightning magnitudes can be expected. However, it can be worth considering the use of more than one active gap arrester rather than just one gapless arrester at the GIS entrance if the required protection zone is to be greater than 86.7 m or if it is economically justifiable. Also, the energy handling capability of the arrester rapidly becomes a crucial factor, as the probability of higher magnitude lightning increases. As an example, in the case of SiC, the energy capability is typically 1.4 kJ/kV of arrester rating [2]. Such an arrester, therefore, can not handle lightnings greater than about 25 kA on systems operating at 400 kV or less, and the use of more than one arrester could become a necessity. Table 8 (for the system in Fig. 11, but with 0.1 H inductive source) emphasizes this aspect, as reflections from the nearby source produce even higher energies and currents.

2.5. Effect of cable connections

Figure 12 shows a circuit configuration that includes a cable connecting the GIS to the overhead line. The last row of Table 10 shows the overvoltages that occur at locations 1, 2 and 3, when no arresters are connected to the system considered, which reach the value of 9.15 pu. Comparison with the case of the system configuration shown in Fig. 2, with no arrester connected (where the overvoltages reach the value of 10.89 pu), shows that the presence of a cable at the GIS entrance

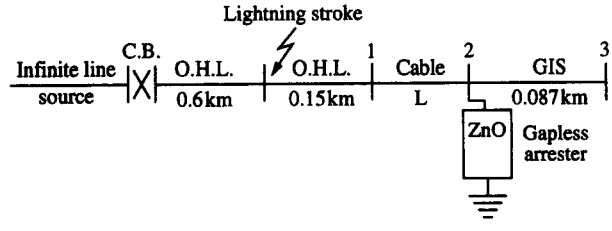

Fig. 12. System under study (with cable).

Table 9. Effect of the cable connected to GIS entrance on its voltages with an active gap (SiC) arrester connected at its entrance (inductive source)

Cable length (km)	Voltages at different points (pu) U_1	U_2	U_3	Arrester energy (kJ)	Arrester current (kA)
0.05	3.35	3.0	3.65	181	8.7
0.1	3.25	3.0	3.56	180	8.5
0.15	3.35	3.05	3.5	175	9.98

Table 10. Effect of connecting arresters at different positions on cable and GIS terminal voltages and arrester stresses (with infinite line source)

Arrester location	Active gap (SiC) arrester									Gapless (ZnO) arrester								
	U_1 (pu)	U_2 (pu)	U_3 (pu)	E_1 (kJ)	C_1 (kA)	E_2 (kJ)	C_2 (kA)	E_3 (kJ)	C_3 (kA)	U_1 (pu)	U_2 (pu)	U_3 (pu)	E_1 (kJ)	C_1 (kA)	E_2 (kJ)	C_2 (kA)	E_3 (kJ)	C_3 (kA)
1	3.05	3.08	3.17	134.5	9.51	—	—	—	—	2.43	2.8	2.89	121.6	14.1	—	—	—	—
2	3.16	3.03	3.38	—	—	134.5	9.12	—	—	2.51	2.38	2.83	—	—	121.6	10.68	—	—
3	3.37	3.29	3.12	—	—	—	—	134.7	10.71	2.97	2.92	2.43	—	—	—	—	121.8	13.53
1 and 2	2.76	2.73	2.87	65.3	5.2	66.0	4.95	—	—	2.25	2.31	2.79	58.7	5.55	60.7	7.6	—	—
1 and 3	2.74	2.74	2.7	65.0	5.02	—	—	66.2	4.65	2.29	2.38	2.23	58.6	7.11	—	—	61	5.16
2 and 3	2.81	2.77	2.71	—	—	65.5	5.31	65.8	4.74	2.39	2.29	2.22	—	—	59.5	6.8	60	4.79
No arrester	9.07	9.04	9.15	—	—	—	—	—	—	9.07	9.04	9.15	—	—	—	—	—	—

U_1, U_2 and U_3, voltages at cable terminal, cable–GIS entrance bus and GIS end; E_n, energy dissipated by arrester; C_n, arrester current at busbar (n).

Table 11. Effect of GIS and OHL lengths on the GIS voltages with (SiC) arresters located at its ends (0.1 H inductive source)

Arrester location		GIS entrance (1)						GIS end (2)						GIS ends (1 and 2)					
OHL (km)	GIS (km)	U_1 (pu)	U_2 (pu)	E_1 (kJ)	C_1 (kA)	E_2 (kJ)	C_2 (kA)	U_1 (pu)	U_2 (pu)	E_1 (kJ)	C_1 (kA)	E_2 (kJ)	C_2 (kA)	U_1 (pu)	U_2 (pu)	E_1 (kJ)	C_1 (kA)	E_2 (kJ)	C_2 (kA)
0.35	0.013	3.1	3.1	207	9.5	—	—	3.0	3.0	—	—	207	9.5	2.75	2.75	98	5.0	98	5.0
	0.052	3.1	3.25	205	9.5	—	—	3.25	3.0	—	—	205	9.5	2.75	2.75	96	5.0	97	5.0
	0.087	3.25	3.75	200	12.2	—	—	3.4	3.1	—	—	200	10.4	2.75	2.75	91	4.9	97	5.25
3.5	0.013	3.1	3.0	271	9.6	—	—	3.0	3.0	—	—	271	9.6	2.75	2.75	135	5.0	135	5.0
	0.052	3.1	3.1	270	9.9	—	—	3.0	3.0	—	—	270	9.75	2.75	2.75	133	5.0	135	5.0
	0.087	3.25	3.8	262	11.7	—	—	3.5	3.1	—	—	264	10.75	2.75	2.75	127	5.25	134	5.3

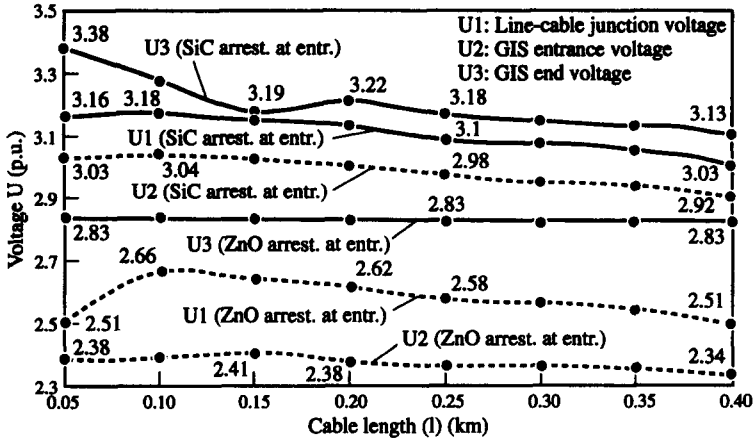

Fig. 13. Effect of length of cable connected to GIS on its overvoltages, arresters connected at GIS entrance (infinite line source).

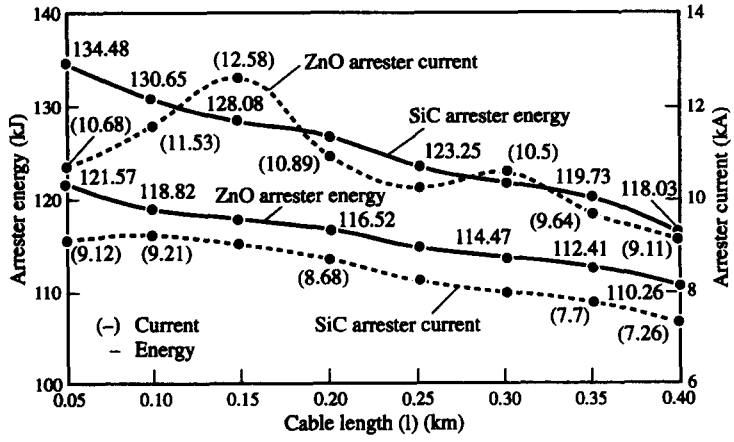

Fig. 14. Effect of the cable length on the arrester energy and current, an arrester connected at the GIS entrance (infinite line source).

reduces the severity of overvoltages. In Fig. 12, when an active gap and a gapless arrester have been connected at the cable end (GIS entrance), respectively, the results given in Figs 13 and 14 show that the overvoltages for a given length of cable would not be easily predicted. The general pattern of results does show, however, that overvoltages tend to decrease as the length of cable is increased. This trend is even more apparent for cable lengths greater than 150 m, although, in the case of a ZnO arrester connected, the open-end overvoltage is unaffected by longer cables. Analysis of current peaks, on the other hand, suggests that disruption by the lightning stroke of energy transmission increased at first for cable lengths up to about 150 m, then decreased significantly. The low surge impedance of cables reduces the magnitude of the wave transmitted into the GIS. Therefore, the presence of a cable at the GIS entrance has a certain benefit and increases the protection zone; thus, fewer arresters are then required. Table 9, for which an inductive power source is added, confirms that, in cases where cable lengths are less than 150 m, overvoltages are somewhat less than easily predictable. Different locations for arresters, however, can possibly modify the above findings. It should also be mentioned that energies decreased significantly, as cable lengths increased, or rather, that they are absorbed over a longer period, as study of "residual" currents would demonstrate.

Table 10 shows the effect of connecting arresters alternatively at the three different locations shown in Fig. 12 (with cable length of 50 m). The protected zone varies accordingly and the best locations should be determined relative to the equipment protected. Table 11 shows the effect

Table 12. Effect of GIS length with transformer connected at its end on its voltages with an arrester connected at GIS end (infinite line source)

	Active gap (SiC) arrester				Gapless (ZnO) arrester			
GIS length (km)	U_1 (pu)	U_2 (pu)	Energy (kJ)	Current (kA)	U_1 (pu)	U_2 (pu)	Energy (kJ)	Current (kA)
0.013	3.02	3.04	136.24	9.0	2.38	2.51	122.97	10.96
0.026	3.09	3.23	135.94	10.28	2.41	2.77	122.73	12.78
0.052	3.12	3.35	135.63	10.84	2.43	2.98	122.5	13.82
0.069	3.14	3.47	135.32	11.21	2.44	3.14	122.27	14.65
0.087	3.15	3.52	135.17	11.51	2.45	3.21	122.15	14.96

Table 13. Effect of GIS length with transformer connected to its end and two (SiC) arresters connected to its ends on its voltages (infinite line source)

	Entrance voltage	End voltage	Entrance arrester		End arrester	
GIS length (km)	U_1 (pu)	U_2 (pu)	Energy (kJ)	Current (kA)	Energy (kJ)	Current (kA)
0.013	2.7	2.7	66.13	4.59	66.36	4.6
0.026	2.7	2.7	65.79	4.63	66.48	4.63
0.052	2.7	2.71	65.42	4.64	66.64	4.76
0.069	2.71	2.73	65.0	4.68	66.83	4.97
0.087	2.7	2.74	64.79	4.63	66.93	5.08

Table 14. Effect of connected transformer to GIS end with active gap (SiC) arresters allocated at different positions on voltages (infinite line source)

	Entrance voltage	End voltage	Arrester 1		Arrester 2	
Arrester location	U_1 (pu)	U_2 (pu)	Energy (kJ)	Current (kA)	Energy (kJ)	Current (kA)
1	2.99	3.5	136	8.4	—	—
2	3.4	2.99	—	—	136	8.35
1 and 2	2.7	2.75	65	4.44	68	5.2

of varying arrester locations when no cable is connecting the OHL and GIS, as shown in Fig. 6 (with OHL of 600 m connected to the source through the C.B.).

2.6. Effect of transformer connections

Tables 12–14 concern a circuit configuration comprising no cables but with a transformer at the GIS open end, for the system shown in Fig. 15. Transformers are represented by their surge capacitance to earth (positive sequence as well as zero sequence capacitance are specified). Comparison of the results of Figs 3 and 4 with Table 12 shows the connection of a transformer caused higher overvoltages to be produced in the GIS and, therefore, reduced protection zones. In addition, the severity of overvoltages for GIS lengths greater than 260 m should be investigated for comparison with Fig. 3, for which transformers are not considered. Comparison of the results in Fig. 5 and the results in Table 13 (with two arresters connected), however, shows that this increase is very much less significant if an additional arrester has been connected at the open-circuited end. Otherwise, previous discussions about Figs 3–5 are also valid with regard to Tables 12 and 13,

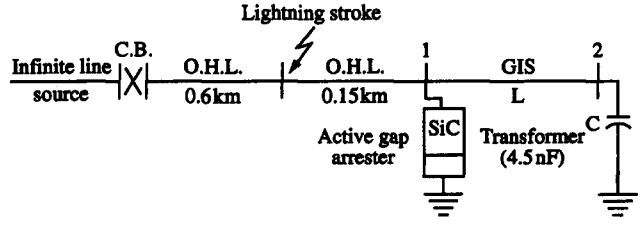

Fig. 15. System under study (with transformer).

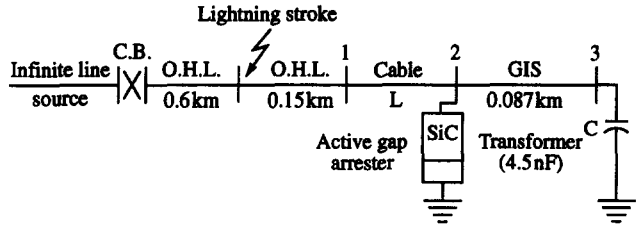

Fig. 16. System under study (cable and transformer).

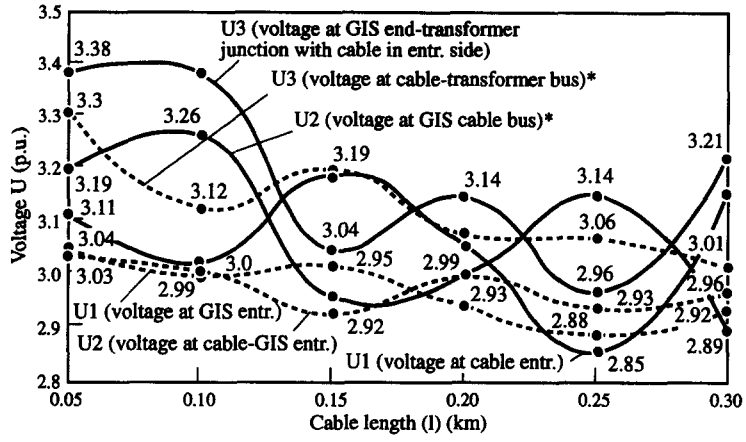

Fig. 17. Effect of cable position and length with transformer connected, an SiC arrester connected at GIS entrance (infinite line source).

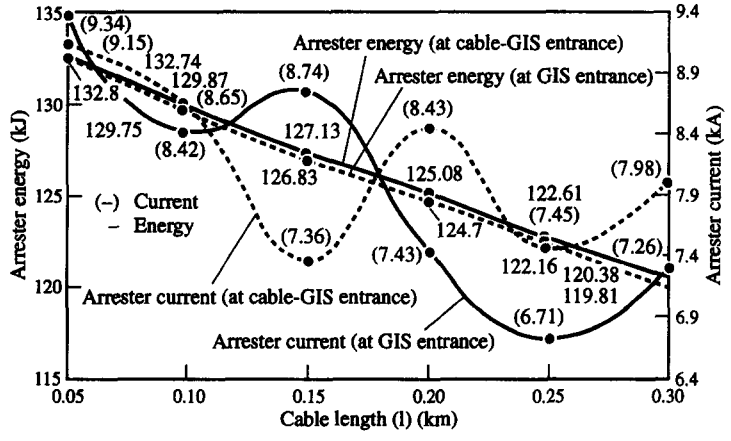

Fig. 18. Effect of cable position and length with transformer connected, an SiC arrester connected at GIS entrance (infinite line source).

respectively. In some cases, however, the presence of a transformer caused slightly reduced rather than higher overvoltages, especially when the GIS length is between 52 and 86.7 m. Compare, for instance, the values in Fig. 3 with the values given in row 8 of Table 12, and the values given in Fig. 5 with the corresponding values in Table 13. For Table 14, arresters are placed at either or both of locations 1 and 2 of Fig. 15.

In the case of the system shown in Fig. 16 and the results given in Figs 17 and 18, the circuit representation comprises both a cable at the GIS entrance and a transformer at its open end. Increased cable length caused a certain but rather erratic reduction in overvoltages. The same phenomena can be observed from the other results given in Figs 17–20 for the systems where the

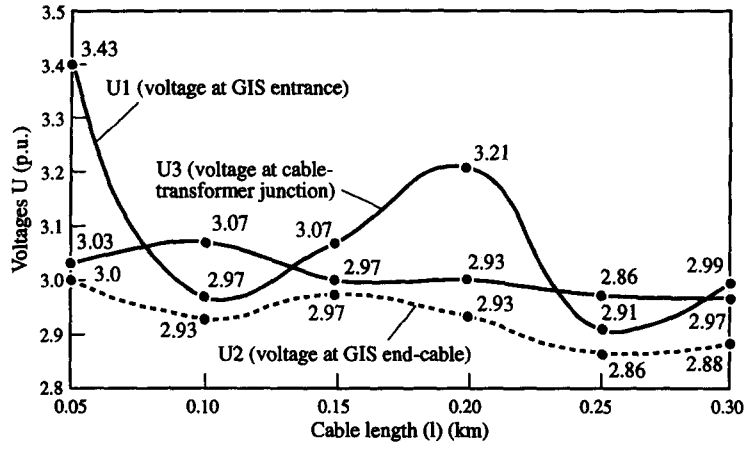

Fig. 19. Effect of cable length and position with transformer connected, an SiC arrester connected at GIS end (infinite line source).

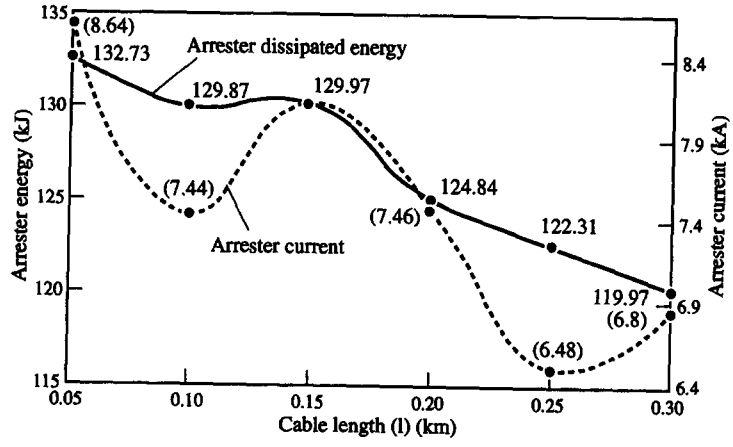

Fig. 20. Effect of cable position and length with transformer connected, an SiC arrester connected at GIS end (infinite line source).

cable lies between the GIS and transformer. This confirms the slight trends in Tables 12 and 13 where the connection of a transformer at the open end of the given system configurations caused lower as well as higher overvoltages.

In Figs 21 and 22 on the other hand, an overhead transmission line is connected between the GIS and the transformer terminal, and an active gap arrester is placed at the GIS entrance and GIS end, respectively. Comparison of Figs 17–20 and 22 with row 5 of Table 12 shows that the introduction of either a cable or an overhead line between the GIS and transformer has a beneficial effect in reducing overvoltages inside the GIS. The high overvoltages that occur at the transformer terminals, however, point out the need for a further surge arrester at this connection. The use of gapless ZnO arresters can perhaps be investigated to achieve eventual economies. From Fig. 22,

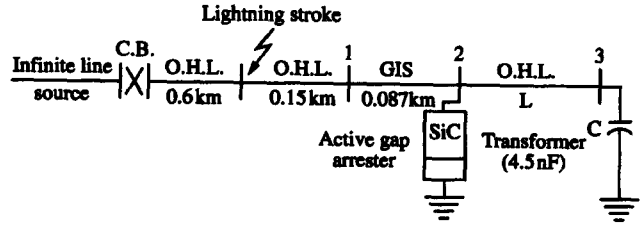

Fig. 21. System under study (O.H.L. and transformer).

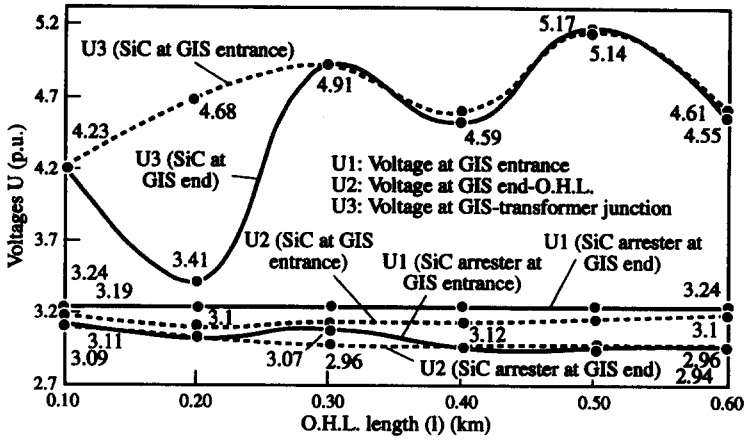

Fig. 22. Effect of O.H.L. position and length with transformer connected, SiC arresters connected at GIS ends (infinite line source).

Table 15. Effect of connecting arresters at different positions on cable and GIS terminal voltages and arrester stresses (0.1 H inductive source)

	Active gap (SiC) arrester							Gapless (ZnO O) arrester						
Arrester location	U_1 (pu)	U_2 (pu)	U_3 (pu)	E_1 (kJ)	C_1 (kA)	E_2 (kJ)	C_2 (kA)	U_1 (pu)	U_2 (pu)	U_3 (pu)	E_1 (kJ)	C_1 (kA)	E_2 (kJ)	C_2 (kA)
1	3.05	3.2	3.4	182	10.0	—	—							
2	3.3	3.0	3.6	—	—	182	8.6	2.6	2.5	3.15	—	—	155	12.0
1 and 2	2.8	2.8	3.25	85	5.6	86	5.2							

U_1, U_2 and U_3, voltages at cable terminal, cable–GIS entrance bus and GIS end; E_n, energy dissipated by arrester; C_n, arrester current at busbar (n).

Table 16. Effect of connected cable length between GIS and transformer on the voltages with (SiC) arresters at different locations (infinite line source)

Arresters location	Cable length (km)	U_1 (pu)	U_2 (pu)	U_3 (pu)	E_1 (kJ)	C_1 (kA)	E_2 (kJ)	C_2 (kA)	E_3 (kJ)	C_3 (kA)
1	0.05	3.1	3.15	3.15	132	10.25	—	—	—	—
2	0.05	3.21	3.1	2.95	—	—	134	9.4	—	—
2	0.1	2.91	2.97	2.9	—	—	130	8.0	—	—
3	0.05	3.41	3.11	2.98	—	—	—	—	132.8	8.25
1 and 2	0.05	2.7	2.75	2.7	64	4.45	66	4.6	—	—
1 and 3	0.05	2.65	2.72	2.74	63.2	4.13	—	—	66.7	5.06
2 and 3	0.05	2.75	2.7	2.65	—	—	65	4.5	66	4.25

U_1, U_2 and U_3, voltages at GIS entrance, GIS end cable and cable–transformer buses, respectively; E and C, energy and current of that bus arrester.

Table 17. Effect of connected OHL length between GIS and transformer on the voltages with (SiC) arresters at different locations (infinite line source)

Arresters location	OHL length (km)	U_1 (pu)	U_2 (pu)	U_3 (pu)	E_1 (kJ)	C_1 (kA)	E_2 (kJ)	C_2 (kA)	E_3 (kJ)	C_3 (kA)
1	0.1	2.94	3.19	4.23	135.1	7.6	—	—	—	—
2	0.1	3.25	3.13	3.75	—	—	136	10.9	—	—
2	0.2	3.25	3.1	4.75	—	—	136	10.0	—	—
3	0.1	4.79	4.63	3.05	—	—	—	—	136.4	9.35
1 and 2	0.1	2.74	2.84	3.44	66	4.75	68	6.1	—	—
1 and 3	0.1	2.94	3.08	2.66	65.3	7.6	—	—	66.7	4.25
2 and 3	0.1	3.25	2.87	2.54	—	—	66	6.48	67	4.22

U_1, U_2 and U_3, voltages at GIS entrance, GIS end OHL and OHL–transformer buses, respectively; E and C, energy and current of that bus arrester.

increasing the OHL length has the effect of smoothing the erratic variations of overvoltage level observed in the case of cables (Figs 17 and 18) and allows for more predictable and reliable overvoltage lowering inside the GIS.

Finally, the effects of changing the locations of the arresters in Fig. 12 (with OHL of 11.85 and 0.15 km and cable of 50 m with inductive source), Fig. 16 (with the cable between the GIS and transformer) and Fig. 21 are shown in Tables 15–17, which confirm most of the findings of the above discussion where relevant.

3. CONCLUSIONS

The results obtained from the different cases studied in this work show the following.

(1) There is an optimum GIS length of 260 m up to which overvoltages increase. They then decrease as the length is further increased.

(2) Increasing GIS length means that arresters are submitted to greater stress due to higher peak currents, up to 260 m.

(3) Energy is dissipated over a longer time period as the GIS length is increased.

(4) Gapless metal oxide (ZnO) arresters are more effective than active gap silicon carbide (SiC) arresters, and their use can result in greater economics, especially since their increasing production and popularity now results in lower prices. Gapless arresters based on non-linear metal oxide varistor blocks provide better overvoltage protection than conventional arresters. In contrast to the active gap sure arrester, the metal oxide arrester conducts a rather high current at voltages far below the nominal protection level, resulting in reduced overvoltage steepness and, consequently, reduced overvoltage amplitudes in the substation. The metal oxide arrester also gives rise to a more linear overvoltage distribution along the GIS, which, in itself, will lower the risk of failure. The lack of a sparkover transient is also a benefit, since that may cause increased overvoltages in the station.

(5) Only the closest of back-flashovers are likely to cause serious concern with respect to insulation coordination.

(6) The effect of switching in some inductive power sources nearby the GIS has to be studied to ensure constant reliability.

(7) The steeper lightning strokes cause the higher overvoltages.

(8) The energy absorption capacity of arresters has to be considered carefully if high magnitude lightnings are expected to occur.

(9) Cable connections reduce overvoltages inside the GIS, to an extent which depends on their length.

(10) Connection of transformers, on the whole, caused higher overvoltages, but lower levels are also recorded.

(11) For GIS systems that are connected to both cables and transformers, it would be necessary to consider every possible switching configuration in order to determine the worst case.

(12) Connected cables or OHL between the GIS and transformer makes it necessary to add some protective device for the benefit of the transformer.

Overall, it can be concluded that the results presented in this work are somewhat overly pessimistic. However, the observed trends could be studied further and a general theory derived that could perhaps predict the effect of different switching configurations on a particular system. This should be done very carefully however, otherwise there is a chance that a low-cost design, acceptable on the basis of a probabilistic method, might be rejected. It is suggested, therefore, that more useful results would be obtained by including statistical calculations. For example, time delays before arrester sparkover in practice cause the active spark gaps to start conduction of current at higher voltages for the faster build-up voltages, whereas the computer program used in this work considered a fixed sparkover level of 1.8 pu. Finally, it is suggested that different bias conditions should be investigated—in particular, the case where phase angles are set to 270, 150 and 300 degrees, for which reflections at an open circuit on phase "a" might cause higher overvoltages.

REFERENCES

1. E. Openshaw, *Power System Transients*. George Newnes Books, New York.
2. U. Ragaller, *Surges in High Voltages Network*. Plenum Press, New York 1979.
3. CIGRE, *Electrical World* (USA) **194**(2), 72 (1980).
4. ERA, *Surge Phenomena*. The British Electrical and Allied Industries Research Association, London (1941).
5. W. Boeck and K. Pettersson, Fundamentals and specific data of Metal-Enclosed substations for the insulation coordination, CIGRE, paper 23-03, Aug. 1978.
6. H. W. Anderl, C. L. Wagner and T. H. Dodds, *IEEE Trans.* **92**(5), 1622 (1973).
7. W. Boeck and H. Troger, SF_6 insulated switchgear for ultra high voltages (UHV), CIGRE 23-08, 1972 session.
8. A. Gromire and G. Voisin, Behaviour of SF_6 metal clad substations subjected to rated currents and heavy fault currents, CIGRE, paper 23-06, Aug. 1978.
9. W. Boeck, In *BBC Symposium on Surges in High Voltage Networks* (ed. K. Rayalles). Plenum Press, New York (1979).
10. K. Azumi, H. Kuwahara, I. Sakon *et al.*, *IEEE Trans.* **99**(3), 947 (1980).
11. G. Carrara, A. Clerici *et al.*, *IEEE Trans.* **88**, 1449 (1969).
12. E. C. Sakshaug *et al.*, "Requirements on EHV and UHV surge arresters, comparison of energy and current duties between field and laboratory conditions by means of TNA simulation", CIGRE paper 33-10, 1976.
13. D. P. Carrol *et al.*, *IEEE Trans.* **91**, 1057 (1972).
14. IEEE Working Group, *IEEE Trans.* **100**, 4033 (1981).
15. T. A. Shami and J. P. Bickford, Some aspects of modelling surge diverter characteristics, 17th Universities Power Engineering Conference, Manchester, England, 30 March–1 April 1982.
16. EPRI-EL-2876, Research project 142-1, final report, "Metal-Oxide surge arresters for Gas-Insulated systems, phases I and II", Feb. 1983, BROWN BOVERI Electric Inc.
17. "Gapless Surge Arresters for Power Systems Applications (Development, Testing, Applications) of 500- and 1200 kV arresters", EL-3166, Vol. 1, 2, 3, research project 657-1, final report, Sept. 1983.
18. A. H. Hamza, PhD thesis, UMIST, U.K. (1987).
19. McGraw-Edison Company, EPRI Final Report EJ1647, Franksville, WI (1980).
20. U. Burger and R. Greuter, *Brown Boveri Rev.* **60**(4), 153 (1973).
21. K. Regallar, *Surges in High Voltages Networks*. Plenum Press, New York (1980).
22. W. Diesendore, *Overvoltages in High Voltages Systems*. The Rensselaer Bookstore, Troy, NY (1971).
23. D. F. Oakeshott, Lightning overvoltages on transmission systems, Power System Overvoltages Symposium, UMIST, U.K., 2–6 September 1974.

APPENDIX

The following data are used in the investigations.

Operating base voltage = 400 kV, one per unit (pu) voltage = $400\sqrt{2}/\sqrt{3} = 326.6$ kV, overhead transmission lines, cables, busbars, and SF_6 GIS are assumed to be lossless and distortionless. Transmission lines and cable surge impedances are

$$Z = \begin{vmatrix} 364.26 & 108.0 & 68.25 \\ 108.0 & 366.65 & 109.6 \\ 68.25 & 109.6 & 352.41 \end{vmatrix} \Omega \quad \text{and} \quad Z = \begin{vmatrix} 30.0 & 0.0 & 0.0 \\ 0.0 & 30.0 & 0.0 \\ 0.0 & 0.0 & 30.0 \end{vmatrix} \Omega$$

while the GIS surge impedance is

$$Z = \begin{vmatrix} 60.0 & 0.0 & 0.0 \\ 0.0 & 60.0 & 0.0 \\ 0.0 & 0.0 & 60.0 \end{vmatrix} \Omega$$

The travelling wave velocity in the lines, cables and GIS are taken as 0.3, 0.15 and 0.26 km/μs, respectively. Source shunt inductance = 0.1 H. Transformer shunt capacitance = 0.0045 μfarad. Active gap surge arresters: $k = 680.0$, $n = 0.17$, sparkover voltage is set to 1.8 pu, maximum gap voltage is 0.8 pu, the time interval between sparkover and start of rise of gap voltage is set to 300 μs, and the build-up time of gap voltage is set to 400 μs. Gapless surge arresters: $k = 631.68$, $n = 0.087$. The standard lightning surge waveform is 1.2/50, with a standard magnitude of voltage generated on the overhead line of 6 pu, where not specified.